경사진 평판형 밀폐 공간에서의 자연 대류 현상의 수치 해석

Numerical Analysis of Natural Convection in Inclined Flat Plate Enclosures

김 용 현* · 고 학 균* · 노 상 하*

Kim, Yong Hyun Koh, Hak Kyun Noh, Sang Ha

적 요

경사진 밀폐 공간에서 마주 보는 두 벽면의 온도 차로 인하여 발생되는 자연 대류 현상은 여러 공학 분야에서 볼 수 있는 중요한 열전달 현상으로서, 최근 들어 평판형 태양열 집열기를 설계하려는 사람들에게 많은 관심의 대상이 되고 있다. 평판형 태양열 집열기의 경우 덮개판으로 부터의 대류 열손실을 감소시킴으로서 집열 효율을 높일 수 있을 뿐만 아니라 사용목적에 따라 소형 집열기를 제작할 수 있어 경제적으로 유리하게 될 것이다.

밀폐된 공간에서 최초에 정지 상태에 있는 얇은 유체층을 하부에서 가열시켜 주면 열팽창 현상이 일어나고, 이것에 의한 부력이 점도나 열전도도 등의 안정화 요인을 극복할 수 있을 정도로 커지면 System이 불안정하게 되어 자연 대류 현상이 수반되며 이 때문에 열전달율이 급격히 증가하게 된다. 이러한 현상의 지배 방정식은 연립 비선형 편미분 방정식으로 특수한 경계 조건외에는 일반적으로 해석적 해를 구하기가 어렵기 때문에 실험적 연구가 많이 실시되어 왔고 이들 결과의 대부분은 전반적인 열전달 특성치만을 구하는데 집중되어 왔다.

본 연구에서는 수치 해석법의 하나인 유한 차분법을 도입하여 이차원으로 가정한 경사진 평판형 밀폐 공간에서의 자연 대류 현상의 지배 방정식을 유한 차분화시켜, $2.74\times10^3 \leqq Gr \leqq 2.0\times10^6$, $Pr=0.73$, $15^\circ \leqq \alpha \leqq 150^\circ$, 종횡비는 1, 2, 3, 5, 9에 대하여 정상 상태에서의 해를 구하면서 수치적으로 실험하였다.

본 연구에서 얻어진 결론을 요약하면 다음과 같다.

(1) 해석적으로 구하기 어려운 경사진 밀폐 공간에서 자연대류현상의 지배 방정식을 유한 차분법으로 해결할 수 있으며, 대류항과 확산항을 따로 고려한 유한차분법이 효과적임을 확인하였다.

(2) 저온과 고온 벽면에서의 온도를 각각 균일하게 놓고 단변으로 이루어진 벽면은 완전히 절연되어 있는 경우에 대하여 수치해를 구한결과, 이전의 해석적 및 실험적 결과와 일치하였으며, 시간의 경과에 따른 온도 및 유선의 변화를 현상학적으로 관찰할 수 있었다.

(3) 평균 열전달 계수에 미치는 경사각의 효과를 살펴본 결과 종횡비가 1인 경우 경사각이 45°에서, 종횡비가 2, 3, 5, 9인 경우 경사각이 60°에서 각각 평균 열전달 계수 최대치가 나타났다.

(4) Ra수(Rayleigh number)가 증가될수록, 경사각에 상관없이 평균 열전달 계수도 증가되었다. 한편 Ra수 및 경사각의 변화에 따라 종횡비가 증가될수록 평균 열전달 계수는 경사각이 90°인 경우를 제외하고는 감소됨을 볼 수 있었다. 경사각이 90°인 경우, 평균 열전달 계수는 종횡비가 2인 곳에서 최대치를 얻을 수 있었으며, 종횡비가 계속 증가될수록 평균 열전달 계수는 점차 감소되어짐을 볼 수 있었다.

NOTATION

a = mesh aspect ratio, $= \Delta X/\Delta Y$

AR = ratio of cavityheight to its width, $= H/L$

C = constant

Cp = specific heat

g = acceleration due to gravity

Gr = Grashof number, $= g\beta(\theta_2-\theta_1)L^3/\nu^2$

h = local heat transfer coefficient, $= -q/(\theta_2-\theta_1)$

H = height of enclosures

*서울대학교 農科大學 農業機械專攻

k = thermal conductivity
L = width of enclosures
Nu = local value of Nusselt number
Nu = mean value of Nusselt number
p = pressure
P = dimensionless pressure deviation, = $p^*L^2/\rho\nu^2$
Pr = Prandtl number, = $\mu Cp/k$
q = heat flux density
Ra = Rayleigh number, = GrxPr
t = time
T = dimensionless temperature, = $(\theta-\theta_o)/(\theta_2-\theta_o)$
u = velocity in the x-direction
U = dimensionless velocity in the X-direction, = uL/ν
v = velocity in the y-direction
V = dimensionless velocity in the Y-direction, = vL/ν
w = velocity vector, = iu + jv
W = length of enclosures in z-direction
x = horizontal coordinate
X = dimensionless horizontal coordinate, = x/L
y = vertical coordinate
Y = dimensionless vertical coordinate, = y/L

Greek Letters

Δx = grid spacing in the x-direction
Δy = grid spacing in the y-direction
$\Delta\tau$ = time increment
α = enclosures tilt angle from horizontal
β = volume coefficient of thermal expansion, = $1/\theta$
ϵ = accuracy check value
ξ = dimensionless vorticity, = $-\nabla^2\psi$
θ = temperature
μ = dynamic viscosity
ν = kinematic viscosity
ρ = density
τ = dimensionless time, = tv/L^2
ψ = dimensionless stream function
ω = relaxation parameter

Mathematical symbols

$\frac{D}{Dt}$ = substantial derivative, = $\frac{\partial}{\partial t}+u\frac{\partial}{\partial x}+v\frac{\partial}{\partial y}$

∇ = vector operator, = $\frac{\partial}{\partial x}+\frac{\partial}{\partial y}$

∇^2 = two-dimensional Laplacian, = $\frac{\partial^2}{\partial X^2}+\frac{\partial^2}{\partial Y^2}$

Subscripts

d = refers to a departure corner
i = denotes to the space subscripts of grid point in the X-direction
j = denotes to the space subscripts of grid point in the Y-direction
p = denotes to the penetration
s = refers to a starting corner
x = refers to the based on x
o = denotes to the initial and static state
1 = refers to the cold plate
2 = refers to the hot plate

Superscripts

n = refers to the number of time steps
k = refers to the number of iterations
* = refers to the perturbation above the static state

I. Introduction

The natural convective heat loss across the enclosed air space heated from the bottom is of interest in many engineering systems. In flat plate solar collectors the natural convective heat loss can constitute the main mode of heat loss. Reduction of heat loss through cover plates will increase collector efficiency and allow smaller collector area to be used.

A phenomena of thermal expansion will occur in a layer of air enclosed which is initially rest and heated from the bottom. If the buoyancy driven by thermal expansion is surpassed the stability factor - viscosity or thermal conductivity - of the fluid, the fluid becomes unstable, and then the heat transfer

rate increases suddenly.

The partial differential equations governing these phenomena are non-linear, and it is hardly surprising that their analytic solution is very difficult or even impossible unless considerable simplifications are made. In an attempt to overcome these difficulties and thereby to extend the range of possible solutions, the finite difference techniques is becoming widely used with the aid of electronic digital computers having high computational speed and large capacity. The purpose of the present work is to examine one particular area of this growing field, viz., that dealing with the finite difference solution of the equations not only of momentum transfer but also of energy transfer, in two dimensional flow.

Indeed, the ultimate aim of this type of work is to find out at least an approximate solution of any analytically intractable problem involving fluid flow and heat transfer.

The specific purpose of this study is:

(1) to develop a finite difference techniques which is applicable for the solution of the simultaneous nonlinear partial differential equations governing the momemtum and heat transfer in inclined flat plate enclosures,

(2) to examine the validity of the techniques by solving a known problem and comparing the results with the existing analytic and experimental results, and

(3) to investigate the effects of the angle of inclination and the aspect ratio of the enclosures on the natural convective heat transfer phenomena inside the enclosures, using the finite difference techniques developed in this study.

II. Review of Literatures

A major concern of solar collector designers is the reduction of heat losses from the hot solar absorber to the cooler environment. Designers seek economic alternatives to minimize these losses, which result from conductive-convective and thermal radiative heat exchanges.

Natural convection in an inclined rectangular region has received increasing attention in recent years.

Batchelor [2] derived the equations governing heat transfer across an air space between two vertical plane boundaries, which is apart distance L, and held at different temperatures. The air space was enclosed by the horizontal plane boundaries, or border strips, distant H apart.

Poots [14] has presented an analytical solution to the steady state cavity wall problem, by expressing temperature and stream function as two doubly infinite series of orthogonal polynomial functions, with appropriate weighting coefficients.

There is a lack of agreement on the effect of aspect ratio on the average heat transfer coefficient. Batchelor [2] has theoretically determined that the boundary effect of enclosures should extend along the heated surface for a distance approximately equal to the plate spacing. This implies that the effect of aspect ratio decreases as aspect ratio increases. Dropkin and Sommerscales [4] have found no effect of aspect ratio in any angles of inclination.

The equations governing the inclined air cells with two side wall boundary conditions, namely that of perfectly insulating and infinitely conducting side walls are solved by Koutsoheras and Charters [7]. They showed that typical curves of mean Nusselt number vs the angle of inclination for the two extreme cases of zero heat flux and linear temperature gradient. Both curves are similar and exhibit maxima at an inclination of about 60 degrees. This agrees with the previous work [10].

An inteferometric study was used to determine the local and average values of the Nusselt number in inclined flat plate enclosures by Randall et al. [15], and Meyer et al. [9] have conducted experiments with air in enclosures of aspect ratios of 0.25 to 4 and tilt angle of 45, 60 and 90 degrees. The results indicate that the convective heat transfer is a strong function of the aspect ratio when the aspect ratio is less than 4.

A numerical methods for solving the simultaneous non-linear partial differential equations governing the conservation of mass, momentum, and energy in problems of natural convection has been studied recently. In the initial investigation, Martini and Churchill [8] measured the temperature and velocity fields for air contained in a long hollow horizontal cylinder with one vertical half heated and the other cooled. They did not complete a numerical solution due to the limitations of the available computer. Thereafter, Hellums and Churchill [5] developed an explicit finite difference method for governing the transient solution to the above problem and also for free convection at a vertical plate.

A finite difference technique has been developed for predicting the transient and steady state natural convection in a rectangular enclosures by Wilkes and Churchill [16]. The governing vorticity and energy transport equations are solved by an implicit alternating direction finite difference method. Transient and steady state isothermals and streamlines are obtained for Grashof numbers up to 100,000 and for aspect ratios of 1, 2 and 3. But they did not report the effects of the angle of inclination and the aspect ratio of the enclosures on the average heat transfer coefficient.

Recently, Ozoe et al. [10-13] investigated natural convection in a long inclined channel with a square cross section and found a minimum and maximum in the heat flux during rotation of the hot plate from the horizontal to the vertical plane about the long axis. They reported good agreement between the experimental average Nusselt number and the one predicted by numerical integration. The minimum heat flux occurred as the angle of inclination was decreased to about 10 degrees, and the maximum heat flux occurred at an inclination of about 50 degrees for all of the Rayleigh numbers which were studied.

III. Governing Differential Equations

A. Problem Statement and basic Equations

The geometrical configuration of flat plate enclosures is shown in Fig. 1. The aspect ratio is assumed to be characterized by H/L only, i.e. W/L is presumed to be enough so that the end walls in the z-direction do not affect the behavior significantly. The top surface of the enclosures was maintained at a constant temperature and the bottom surface also at constant but high temperature than that of the top surface. Let the initial temperature equal the mean of the applied temperatures, so that $(\theta_1 + \theta_2)/2$. The other sides were thermally insulated. The whole enclosures was then rotated about the z-axis.

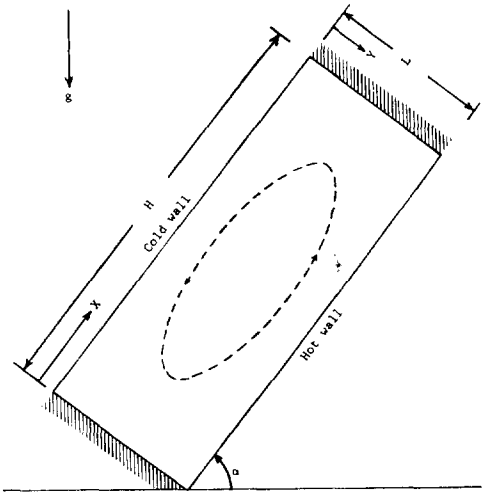

Fig. 1. Geomerical configuration of flat plate enclosures

To formulate the boundary value problem that describes this phenomena it is assumed: (a) the fluid is Newtonian, (b) the motion is two-dimensional and time-dependent, (c) the frictional heating is negligible, (d) the temperature difference between hot surface and cold surface is small compared with the absolute temperatures of the cold surface. This permits so-called the Boussinesq approximation to be invoked, which permits fluid properties to be taken as constant except for the density variation inducing the buoyancy force. Density is taken as a function

of temperature θ according to the equation of state

$$\rho = \frac{\rho_0}{1+\beta(\theta-\theta_0)} \tag{3-1}$$

where, β is a constant. Thus the basic equations are:

$$\nabla w = 0 \tag{3-2}$$

$$\frac{Dw}{Dt} = -\frac{1}{\rho}\nabla p + \nu\nabla^2\omega + \beta g \tag{3-3}$$

$$\rho C\frac{D\theta}{Dt} = k\nabla^2\theta \tag{3-4}$$

The x- and y-components of momentum equation (3-3) are as follows:

$$\frac{\partial u}{\partial t} + u\frac{\partial u}{\partial x} + v\frac{\partial u}{\partial y} = -\frac{1}{\rho}\frac{\partial p}{\partial x} + \nu\left(\frac{\partial^2 u}{\partial x^2} + \frac{\partial^2 u}{\partial y^2}\right) - g\sin\alpha \tag{3-5}$$

$$\frac{\partial v}{\partial t} + u\frac{\partial v}{\partial x} + v\frac{\partial v}{\partial y} = -\frac{1}{\rho}\frac{\partial p}{\partial y} + \nu\left(\frac{\partial^2 v}{\partial x^2} + \frac{\partial^2 v}{\partial y^2}\right) + g\cos\alpha \tag{3-6}$$

If there is no fluid motion in the field, the total pressure is equal to the static pressure. In general the total pressure may be represented as the sum of the static pressure and a perturbation:

$$p = p_o + p^* \tag{3-7}$$

When $u = v = 0$,

$$-\frac{\partial p_o}{\partial x} - \rho_o g\sin\alpha = 0 \tag{3-8}$$

and

$$-\frac{\partial p_o}{\partial y} + \rho_o g\cos\alpha = 0 \tag{3-9}$$

Then,

$$-\frac{1}{\rho}\frac{\partial p}{\partial x} - g\sin\alpha = g\beta(\theta-\theta_o)\sin\alpha - \frac{1}{\rho}\frac{\partial p^*}{\partial x} \tag{3-10}$$

$$-\frac{1}{\rho}\frac{\partial p}{\partial y} + g\cos\alpha = -g\beta(\theta-\theta_o)\cos\alpha - \frac{1}{\rho}\frac{\partial p^*}{\partial y} \tag{3-11}$$

Substituting equations (3-10) and (3-11) into the momentum equations (3-5) and (3-6), we obtain the following forms:

$$\frac{\partial u}{\partial t} + u\frac{\partial u}{\partial x} + v\frac{\partial u}{\partial y} = g\beta(\theta-\theta_o)\sin\alpha - \frac{1}{\rho}\frac{\partial p^*}{\partial x} + \nu\left(\frac{\partial^2 u}{\partial x^2} + \frac{\partial^2 u}{\partial y^2}\right) \tag{3-12}$$

$$\frac{\partial v}{\partial t} + u\frac{\partial v}{\partial x} + v\frac{\partial v}{\partial y} = -g\beta(\theta-\theta_o)\cos\alpha - \frac{1}{\rho}\frac{\partial p^*}{\partial y} + \nu\left(\frac{\partial^2 v}{\partial x^2} + \frac{\partial^2 v}{\partial y^2}\right) \tag{3-13}$$

From equations (3-2) and (3-4), the continuity and energy equation is now exprssed as follows:

$$\frac{\partial u}{\partial x} + \frac{\partial v}{\partial y} = 0 \tag{3-14}$$

$$\frac{\partial\theta}{\partial t} + u\frac{\partial\theta}{\partial x} + v\frac{\partial\theta}{\partial y} = \frac{K}{\rho Cp}\left(\frac{\partial^2\theta}{\partial x^2} + \frac{\partial^2\theta}{\partial y^2}\right) \tag{3-15}$$

Finally, the initial and boundary conditions for the problem are:

$$u(x,y,0) = v(x,y,0) = 0,\ \theta(x,y,0) = \theta o$$

$$u(0,y,t) = u(H,y,t) = v(0,y,t) = v(H,y,t) = 0$$

$$\frac{\partial\theta}{\partial x}(0,y,t) = \frac{\partial\theta}{\partial x}(H,y,t) = 0$$

$$u(x,0,t) = v(x,0,t) = 0,\ \theta(x,0,t) = \theta_1$$

$$u(x,L,t) = v(x,L,t) = 0,\ \theta(x,L,t) = \theta_2$$

Equations (3-12) through (3-15) may now be transformed into non-dimensional form by introducing suitable dimensionless variables.

Non-dimensional form of the equations (3-12) through (3-15) and the boundary conditions are as follows:

$$\frac{\partial U}{\partial X} + \frac{\partial V}{\partial Y} = 0 \tag{3-16}$$

$$\frac{\partial U}{\partial\tau} + U\frac{\partial U}{\partial X} + V\frac{\partial U}{\partial Y} = \frac{Gr\ T\sin\alpha}{2} - \frac{\partial P}{\partial X} + \frac{\partial^2 U}{\partial X^2} + \frac{\partial^2 U}{\partial Y^2} \tag{3-17}$$

$$\frac{\partial V}{\partial\tau} + U\frac{\partial V}{\partial X} + V\frac{\partial V}{\partial Y} = -\frac{Gr\ T\cos\alpha}{2} - \frac{\partial P}{\partial Y} + \frac{\partial^2 V}{\partial X^2} + \frac{\partial^2 V}{\partial Y^2} \tag{3-18}$$

$$\frac{\partial T}{\partial\tau} + U\frac{\partial T}{\partial X} + V\frac{\partial T}{\partial Y} = \frac{1}{Pr}\left(\frac{\partial^2 T}{\partial X^2} + \frac{\partial^2 T}{\partial Y^2}\right) \tag{3-19}$$

$$U(X,Y,0) = V(X,Y,0) = T(X,Y,0) = 0$$

$$U(0,Y,\tau) = U(AR,Y,\tau) = V(0,Y,\tau) = V(AR,Y,\tau) = 0$$

$$\frac{\partial T}{\partial X}(0,Y,\tau) = \frac{\partial T}{\partial X}(AR,Y,\tau) = 0$$

$$U(X,0,\tau) = V(X,0,\tau) = 0, T(X,0,\tau) = -1$$

$$U(X,1,\tau) = V(X,1,\tau) = 0, T(X,1,\tau) = 1$$

Equations (3-16) through (3-19) were not in a suitable form for finite difference computation due to the appearance of pressure in both equations of motion. Differentiating equations (3-17) and (3-18) with respect to Y and X, respectively, subtracting, and substituting equation (3-16) produces the following equation in which pressure term no longer appears:

$$\frac{\partial}{\partial \tau}\left(\frac{\partial U}{\partial Y} - \frac{\partial V}{\partial X}\right) + U\frac{\partial^2 U}{\partial X \partial Y} + V\frac{\partial^2 U}{\partial Y^2} - U\frac{\partial^2 V}{\partial X^2} - V\frac{\partial^2 V}{\partial X \partial Y} = \frac{Gr}{2}\left(\frac{\partial T}{\partial Y}\sin\alpha + \frac{\partial T}{\partial X}\cos\alpha\right) + \frac{\partial(\nabla^2 U)}{\partial Y} - \frac{\partial(\nabla^2 V)}{\partial X} \qquad (3\text{-}20)$$

The introduction of a dimensionless vorticity $\xi = -\nabla^2\psi$, where the dimensionless stream function was such that $U = \partial\psi/\partial Y$ and $V = -\partial\psi/\partial X$, enables the problem to be written as follows:

$$\frac{\partial \xi}{\partial \tau} + U\frac{\partial \xi}{\partial X} + V\frac{\partial \xi}{\partial Y} = -\frac{Gr}{2}\left(\frac{\partial T}{\partial Y}\sin\alpha + \frac{\partial T}{\partial X}\cos\alpha\right) + \nabla^2\xi \qquad (3\text{-}21)$$

$$\frac{\partial T}{\partial \tau} + U\frac{\partial T}{\partial X} + V\frac{\partial T}{\partial Y} = \frac{1}{Pr}\nabla^2 T \qquad (3\text{-}22)$$

$$\nabla^2\psi = -\xi \qquad (3\text{-}23)$$

$$U = \frac{\partial \psi}{\partial Y}, \quad V = -\frac{\partial \psi}{\partial X} \qquad (3\text{-}24)$$

$$\xi(X,Y,\tau) = T(X,Y,\tau) = 0$$

$$\psi(0,Y,\tau) = \frac{\partial \psi}{\partial X}(0,Y,\tau) = \psi(AR,Y,\tau) = \frac{\partial \psi}{\partial X}(AR,Y,\tau) = 0$$

$$\frac{\partial T}{\partial X}(0,Y,\tau) = \frac{\partial T}{\partial X}(AR,Y,\tau) = 0$$

$$\psi(X,0,\tau) = \frac{\partial \psi}{\partial Y}(X,O,\tau) = 0, \quad T(X,0,\tau) = -1$$

$$\psi(X,1,\tau) = \frac{\partial \psi}{\partial Y}(X,1,\tau) = 0, \quad T(X,1,\tau) = 1$$

Equations (3-21) through (3-24) here are called the vorticity transport; temperature, stream function, and velocity equations, respectively. With given the boundary conditions, the above five simultaneous non-linear partial differential equations may be solved and then the dependent variables, T, ξ, ψ, U, and V are obtained.

IV. Finite Difference Method

A. Calculation of Temperature

The basic finite difference formula for partial derivatives can be derived by expanding into Taylor series and taking up to second order terms. In the first system, a Taylor series expansion gives

$$T_{j,i}^{n+1} = T_{j,i}^{n} + \frac{\partial T}{\partial \tau}\Big|_{j,i}^{n}\Delta\tau + \frac{\partial^2 T}{\partial \tau^2}\Big|_{j,i}^{n}\frac{(\Delta\tau)^2}{2} + O(\Delta\tau^3) \qquad (4\text{-}1)$$

If we only consider the convective terms in temperature equation, then equation (3-22) becomes

$$\frac{\partial T}{\partial \tau} = -U\frac{\partial T}{\partial X} - V\frac{\partial T}{\partial Y} \qquad (4\text{-}2)$$

Differentiating equation (4-2) with respect to time, the above equation becomes as following form:

$$\frac{\partial^2 T}{\partial \tau^2} = \frac{\partial}{\partial \tau}\left(-U\frac{\partial T}{\partial X} - V\frac{\partial T}{\partial Y}\right) \qquad (4\text{-}3)$$

Using the forward-time and centered-spaces finite differencing, and substituting equation (4-2) and (4-3) into equation (4-1), then the temperature, $\hat{T}_{j,i}^{n+1}$, considering only convective term at the (n+1) time step is given by

$$\hat{T}_{j,i}^{n+1} = T_{j,i}^{n} - \frac{\Delta\tau}{2\Delta X\Delta Y}[U_{j,i}(T_{j,i+1} - T_{j,i-1})\Delta Y + V_{j,i}(T_{j+1,i} - T_{j-1,i})\Delta X] + \frac{(\Delta\tau)^2}{8(\Delta X)^2(\Delta Y)^2}[2U_{j,i}(U_{j,i+1} - U_{j,i-1})(T_{j,i+1} - T_{j,i-1})(\Delta Y)^2 + 4U_{j,i}^2(T_{j,i+1} - 2T_{j,i} + T_{j,i-1})(\Delta Y)^2 + V_{j,i}(U_{j,i+1} - U_{j,i-1})$$

$$(T_{j+1,i} - T_{j-1,i})\,(\Delta X\Delta Y) + U_{j,i}(V_{j,i+1} - V_{j,i-1})$$

$$(T_{j+1,i} - T_{j-1,i})\,(\Delta X\Delta Y) + 2U_{j,i}V_{j,i}(T_{j+1,i+1} +$$

$$T_{j-1,i-1} - T_{j+1,i-1} - T_{j-1,i+1})\,(\Delta X\Delta Y) + V_{j,i}$$

$$(U_{j+1,i} - U_{j-1,i})\,(T_{j,i+1} - T_{j,i-1})\,(\Delta X\Delta Y) + U_{j,i}$$

$$(V_{j+1,i} - V_{j-1,i})\,(T_{j,i+1} - T_{j,i-1})\,(\Delta X\Delta Y) + 2V_{j,i}$$

$$(V_{j+1,i} - V_{j-1,i})\,(T_{j+1,i} - T_{j-1,i})\,(\Delta X^2)$$

$$+ 4V^2_{j,i}\,(T_{j+1,i} - 2T_{j,i} + T_{j-1,i})\,(\Delta X^2)] \qquad (4\text{-}4)$$

Now adding the conductive term, the complete form of temperature equation is presented as follows:

$$T^{n+1}_{j,i} = \hat{T}^{n+1}_{j,i+1} + \frac{\Delta\tau}{Pr}\left(\frac{\hat{T}^{n+1}_{j,i+1} - 2\hat{T}^{n+1}_{j,i} + \hat{T}^{n+1}_{j,i-1}}{\Delta X^2} + \right.$$

$$\left.\frac{\hat{T}^{n+1}_{j+1,i} - 2\hat{T}^{n+1}_{j,i} + \hat{T}^{n+1}_{j-1,i}}{\Delta Y^2}\right)$$

$$= \hat{T}^{n+1}_{j,i} + \frac{\Delta\tau}{Pr(\Delta X^2)\,(\Delta Y^2)}\,[\,(\hat{T}^{n+1}_{j,i+1} - 2\hat{T}^{n+1}_{j,i} +$$

$$\hat{T}^{n+1}_{j,i-1})\,(\Delta Y)^2 + (\hat{T}^{n+1}_{j+1,i} - 2\hat{T}^{n+1}_{j-i} + \hat{T}^{n+1}_{j-1,i})$$

$$(\Delta X)^2] \qquad (4\text{-}5)$$

The wall temperatures are now obtained from the insulated type of boundary condition. In evaluating these temperatures, it is particularly important to be consistent with the finite difference scheme used at the interior points.

Derivations for the wall temperatures are presented in Kim[1]. The following approximation is obtained for temperature at the insulated wall:

$$T_{j,i} = \frac{1}{3}(4T_{j,i+1} - T_{j,i+2}) \qquad (4\text{-}6)$$

B. Calculation of Stream Field

The vorticity is also obtained by the same method as done in calculation of temperature.

Equation (3-23) is the Poisson form of the stream function. This equation can be solved by method of Richardson, Liebmann, SOR (Successive Over-Relaxation). Using the SOR method, the equation (3-23) may be rewritten as follows:

$$\psi^{k+1}_{j,i} = \psi^{k}_{j,i} + \frac{\omega}{2(1+a^2)}\,[\,(\Delta X)^2\xi^{n+1}_{j,i} + \psi^{k}_{j,i} +$$

$$\psi^{k+1}_{j,i-1} + a^2\psi^{k}_{j+1,i} + a^2\psi^{k+1}_{j-1,i} - 2(1+a^2)\psi^{k}_{j,i}] \qquad (4\text{-}7)$$

In this work the convergence test of three methods for solving the Poisson equation was performed to determine which method would be efficient. Therefore, all of the numerical simulation were made by the efficient method. The criterion of iteration convergence for steady state ψ was given as

$$\max\left|\frac{\psi^{k+1}_{j,i} - \psi^{k}_{j,i}}{\psi^{k+1}_{j,i}}\right| \le \epsilon \qquad (4\text{-}8)$$

where, ϵ was 1.0×10^{-4}.

The new wall vorticities were obtained from the no-slip conditions.

$$\xi_{j,i} = -\frac{2\psi_{j+1,i}}{\Delta Y^2} \qquad (4\text{-}9)$$

Finally, the new velocity fields of U and V were obtained from the centered-spaces finite difference approximation of the velocity equation (3-24) and the wall velocities become zero from the no-slip conditions.

$$U_{j,i} = \frac{\psi_{j+1,i} - \psi_{j-1,i}}{2\Delta Y} \qquad (4\text{-}10)$$

$$V_{j,i} = \frac{\psi_{j,i-1} - \psi_{j,i+1}}{2\Delta X} \qquad (4\text{-}11)$$

C. Local and Mean Nusselt Number

The heat flux at the cold plate Y = 0 is an important quantity, since it equals the rate of heat transfer across the enclosures. Now the local heat flux density at this plate is

$$q = -k\left(\frac{\partial\theta}{\partial y}\right)\Big|_{y=0} = -k\frac{(\theta_2 - \theta_0)}{L}\left(\frac{\partial T}{\partial Y}\right)\Big|_{Y=0} \qquad (4\text{-}12)$$

Since the overall temperature difference between the inclined plates is $(\theta_2 - \theta_1) = 2(\theta_2 - \theta_o)$, a local transfer coefficient may be defined as following:

$$h = -\frac{q}{(\theta_2 - \theta_1)} = \frac{k}{2L}\left(\frac{\partial T}{\partial Y}\right)|_{Y=0} \qquad (4\text{-}13)$$

The corresponding local Nusselt number is

$$Nu_X = \frac{hL}{k} = \frac{1}{2}\left(\frac{\partial T}{\partial Y}\right)|_{Y=0} \qquad (4\text{-}14)$$

The mean Nusselt number over the cold plate of the enclosures was obtained by numerical integration of the local Nusselt number and its value is defined as follows:

$$\overline{Nu} = \frac{1}{H}\int_0^H Nu_x \, dx \qquad (4\text{-}15)$$

The right-hand side of euqation (4-15) was integrated using Simpson's formula.

V. Results and Discussion

A. Conditions for Computer Solution

As the result of a stability analysis using the von Neumann's stability criteria, the following condition was sufficient to ensure stability for the conduction term of the energy equation and the diffuse term of the vorticity transport equation.

$$\frac{\Delta\tau}{Pr}\left(\frac{1}{\Delta X^2} + \frac{1}{\Delta Y^2}\right) \leq \frac{1}{2} \qquad (5\text{-}1)$$

And, for the convective term the following condition was required for limitation of the time increment,

$$\Delta\tau\left(\frac{|U|}{\Delta X} + \frac{|V|}{\Delta Y}\right) \leq 1 \qquad (5\text{-}2)$$

Since the equation (5-1) gives the practical limitation to the time increment, the equation (5-1) was initially used to solve the energy equation and the equation (5-2) limited by convective term was used for the next time steps.

B. Validity of the Results

The most vital question that may be asked about the computed results is that concerning their accuracy. There are three types of check which may be made, viz. (a) a direct comparison with a known analytical solution, (b) a direct comparison with experimental results, and (c) subjection of the computed results to further tests to see if they are reason-

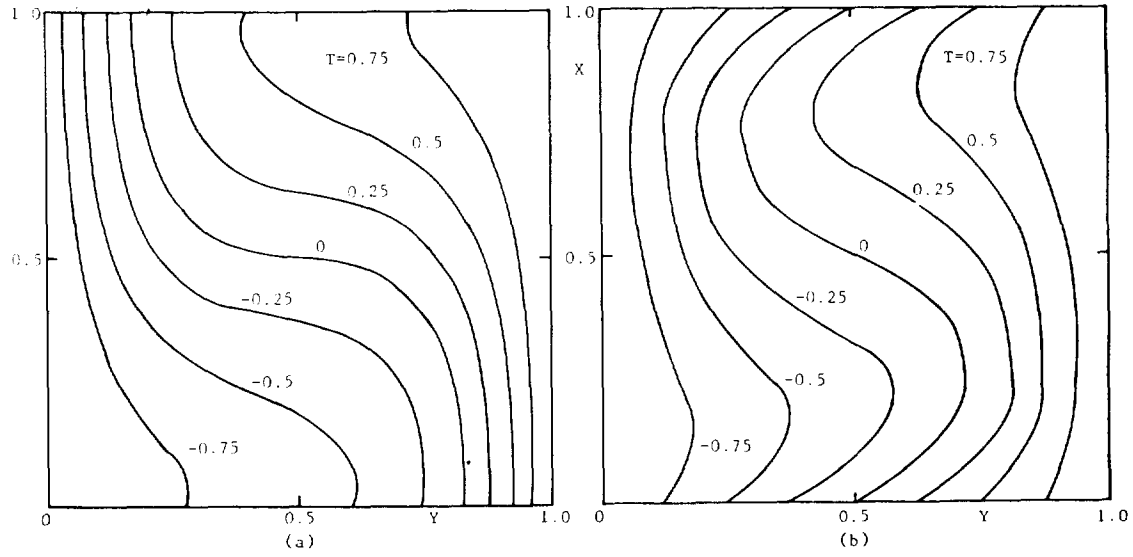

Fig. 2. Comparison of computed steady state isothermals with Poots' analytic solution for AR=1.0, Pr=0.73, Ra=5.0x10³, α=90° : (a) computed solution, insulated (b) Poots' solution, linear

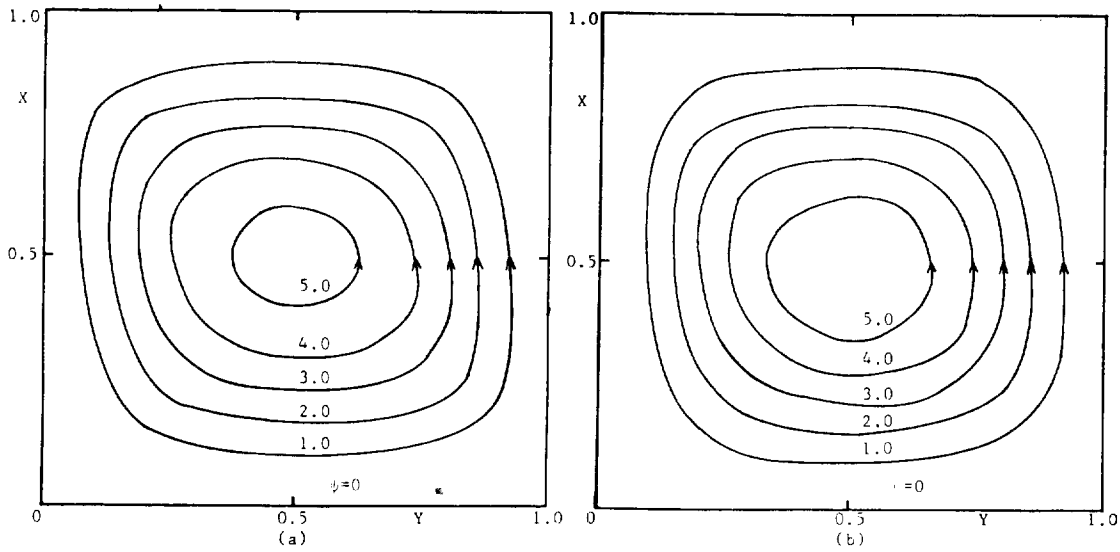

Fig. 3. Comparison of computed steady state streamlines with Poots' analytic solution for AR= 1.0, Pr=0.73, Ra= 5.0×10^3, $\alpha = 90°$: (a) computed solution, insulated (b) Poots' solution, linear

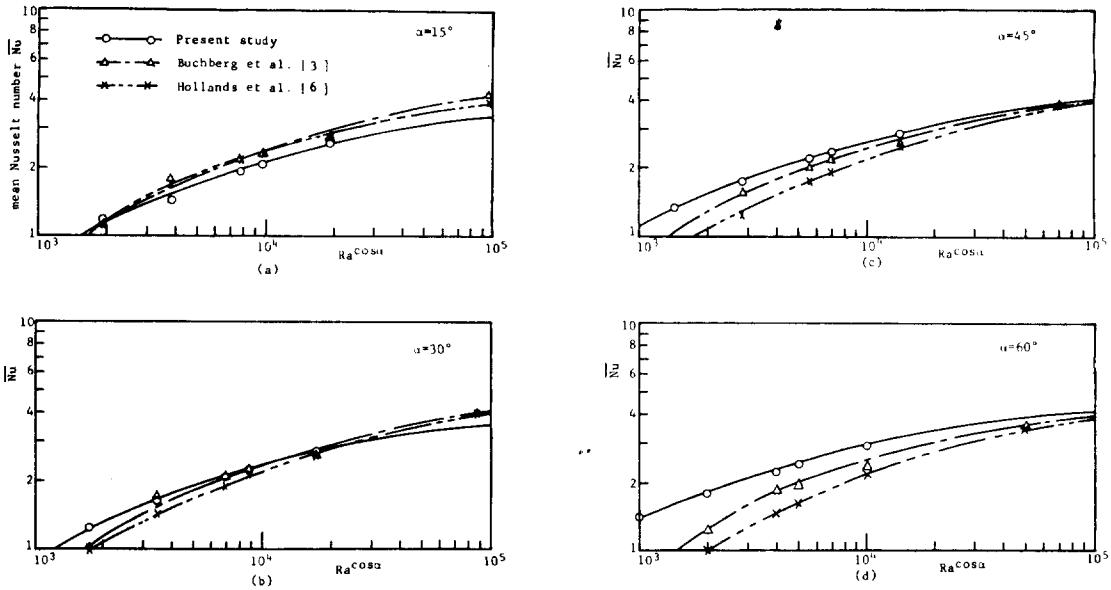

Fig. 4. Comparison of present mean Nusselt number results with those of previous ivestigators : (a) $\alpha = 15°$ (b) $\alpha = 30°$ (c) $\alpha = 45°$ (d) $\alpha = 60°$

able.

Firstly, the finite difference solution for a 11 x 11 mesh was compared with the analytical steady state solution of Poots [14] in the isothermals and streamlines plots as shown Fig. 2 and 3. This coincidence is such as to substantiate the validity of both Poots' and the present values. The streamlines are fairly close and the isothermals are almost identical

except the case in the vicinity of both short walls, which is considered for linear variation of temperature in Poots' analysis.

Secondly, the computed mean Nusselt number, $\overline{Nu}$ under steady state may be compared with the following correlations based on the experiments of Buchberg et al. [3] and Hollands et al. [6].

Buchberg et al. correlations:

$$\overline{Nu} = 1 + 1.446\left[1 - \frac{1708}{Ra\cos\alpha}\right] \text{ for } 1708 \le Ra\cos\alpha \le 5900$$

$$\overline{Nu} = 0.229(Ra\cos\alpha)^{0.252} \text{ for } 5900 \le Ra\cos\alpha \le 9.23 \times 10^4$$

$$\overline{Nu} = 0.157(Ra\cos\alpha)^{0.285} \text{ for } 9.23 \times 10^4 \le Ra\cos\alpha \le 1.0 \times 10^6$$

Hollands et al. correlation:

$$\overline{Nu} = 1 + 1.44\left[1 - \frac{1708}{Ra\cos\alpha}\right]\left(1 - \frac{(\sin 1.8\alpha)^{1.6}\,1708}{Ra\cos\alpha}\right) + \left[\left(\frac{Ra\cos\alpha}{5830}\right)^{1/3} - 1\right] \text{ for } \alpha \le 60 \text{ deg.}$$

It should be noted that brackets in these correlations go to zero when negative. Generally speaking, the values of $\overline{Nu}$ listed in Table 1 lie roughly between 1% and 85% higher than those predicted be these correlations. Perhaps, this comparison cannot be regarded as conclusive one, since the effect of aspect ratio on the mean Nusselt number was excluded. A comparison of present mean Nusselt number with those of investigators is given in Fig. 4.

Table 1. Mean Nusselt number at cold plate for AR=1.0, Pr=0.73, Ra=1.0×10^4, α=90 deg.

τ	$\Delta X=\Delta Y=0.1$		$\Delta X=\Delta Y=0.05$
	$\Delta\tau=0.0005$	$\Delta\tau=0.001$	$\Delta\tau=0.0004$
0.0004	–	–	7.8082
0.0005	4.6575	–	–
0.0008	–	–	6.5772
0.001	4.3620	4.3151	–
0.0012	–	–	5.7805
0.0015	4.1053	–	–
0.0016	–	–	5.2149
0.002	3.8810	3.8177	4.7874
0.003	3.5097	3.4439	–
0.004	3.2166	3.1541	3.5813
0.005	2.9805	2.9234	–
0.01	2.2750	2.2403	2.3620
0.012	2.1135	2.0836	2.1752
0.014	1.9901	1.9633	2.0344
0.016	1.8954	1.8706	1.9236
0.02	1.7703	1.7475	1.7726
0.03	1.7291	1.7089	1.6633
0.04	1.9844	1.9663	1.8539
0.05	2.3166	2.2881	2.1653
0.1	2.4130	2.3719	2.2972
0.15	2.4277	2.3856	2.3087
0.2	2.4263	2.3845	2.3074

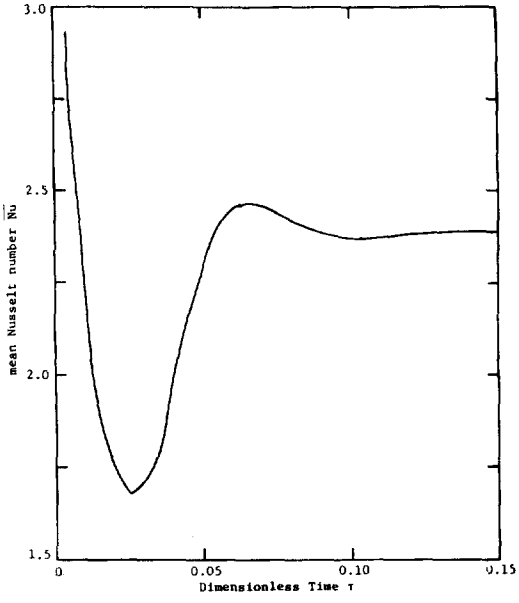

Fig. 5. Variation of mean Nusselt number with time; AR=1, Pr=0.73, Ra=1.0×10^4

Thirdly, it is reasonable to expect that the results computed by the finite difference procedure should satisfy the following requirements:

(a) The steady state solution should be independent of the time increment employed in this study.

(b) A subdivision of the grid spacing should not alter the results greatly.

(c) The use of a smaller time increment should not alter the transient results greatly.

Each of these tests was applied in turn to the results computed for the condition viz. an insulated square cavity, with Pr = 0.73, Gr = 13,699, and $\Delta X = \Delta Y = 0.1$, corresponding to a 11 x 11 mesh. The following results were obtained.

(a) The steady state solutions reached essentially by a time $\tau = 0.25$ were almost the same as two different values of time increment, viz. $\Delta\tau = 0.0025$ and $\Delta\tau = 0.001$.

(b) The computations were repeated for a 21 x 21 mesh, i.e. one with half the original spacing, but the new values of temperature showed little deviation from their values on the 11 x 11 mesh. For example, in passing to the finer grid, the stream function at the center of the cavity changed only slightly, from 7.561 to 7.125. Considering the complexity of the problem, these differences are astonishingly small. These findings, taken in conjuction with the good agreement with Poots' solution, indicate that a 11 x 11 mesh is probbably adequate for the remaining computations of this work. This is very fortunate, especially since the computing time increases rapidly as the mesh is refined.

(c) The effect on the transient mean Nusselt number of changing the time increment from $\Delta\tau = 0.0025$ to $\Delta\tau = 0.001$ is considered to be almost negligible as shown in Table 1.

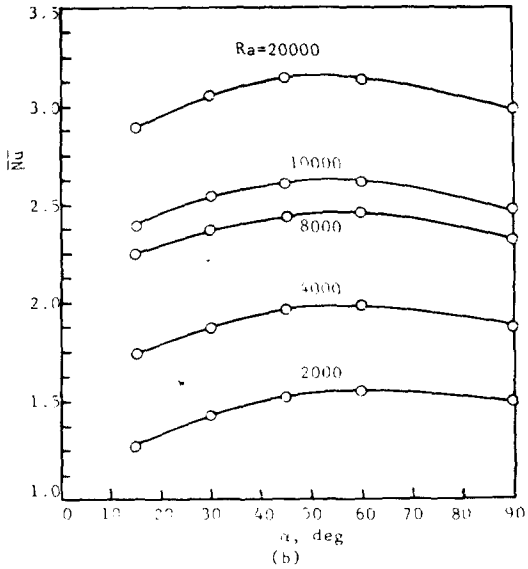

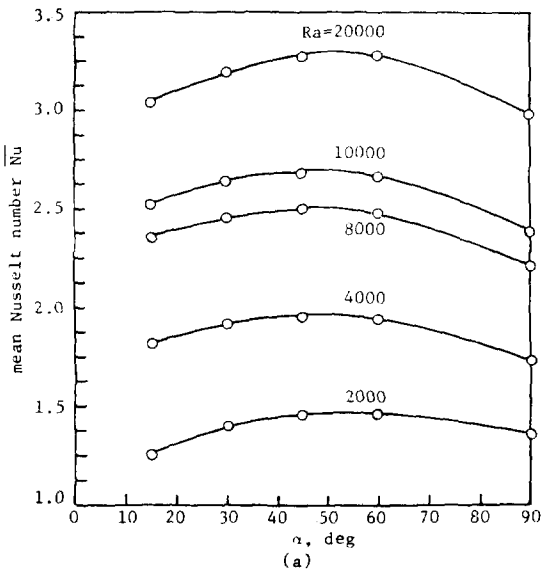

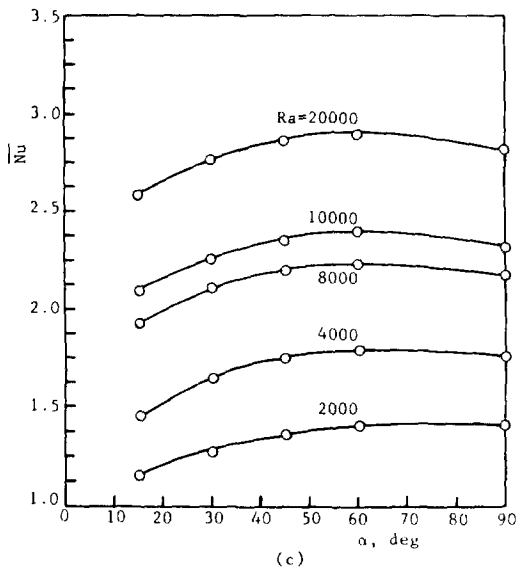

Fig. 6. Computed mean Nusselt numbers vs inclination at various Rayleigh numbers : (a) AR=1.0 (b) AR=2.0 (c) AR=3.0

C. Heat Transfer Across the Enclosures

The variation of the mean Nusselt number $\overline{Nu}$ with time is shown in Table 1 and Fig. 5, for insulated type of boundary condition. Referring to Fig. 5, the mean Nusselt number falls sharply from the initial value and reaches a minimum at about τ = 0.026. During these initial stages, the heat is transferred mainly by conduction, and the fluid velocity accelerates from its original value of zero.

The effect of convective heat transfer become increasingly apparent as time advances beyond τ = 0.026. A small overshoot at τ = 0.066 and an even smaller undershoot at τ = 0.104 are visible from Fig. 5. The computed results showed that the Nusselt number also exhibited further oscillations, but their magnitude decayed very rapidly. The final value of the mean Nusselt number of 2.3845 indicates that convection now predominates over conduction.

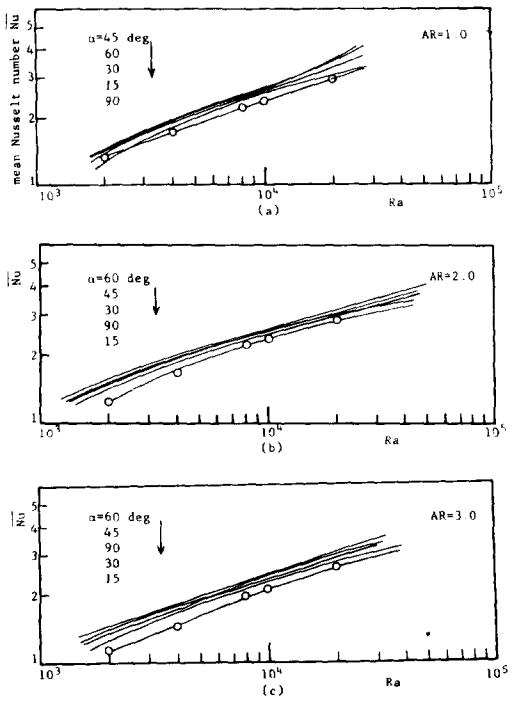

Fig. 7. Computed mean Nusselt numbers vs Rayleigh numbers at various inclination : (a) AR=1.0 (b) AR=2.0 (c) AR=3.0

The effect on the mean Nusselt number of Rayleigh number is illustrated in Figs. 6 and 7 for various aspect ratios of 1.0, 2.0, and 3.0 Referring to Figs. 6 and 7, the maximum mean Nusselt number was found to be occurred at about 45 degrees of inclination for aspect ratio of 1.0 and about 60 degrees of inclination for aspect ratio of 2.0, 3.0, 5.0, and 9.0. These results have a good agreements with the previous experimental results [6,9-12].

The effect on the mean Nusselt number of the aspect ratio is shown in Fig. 8 for various Grashof number and the angle of inclination. For the aspect ratio of 1.0 large Nusselt number was appeared at the angle of inclination less than 60 degrees, and also for the increasing aspect ratio large Nusselt number was appeared at the angle of inclination

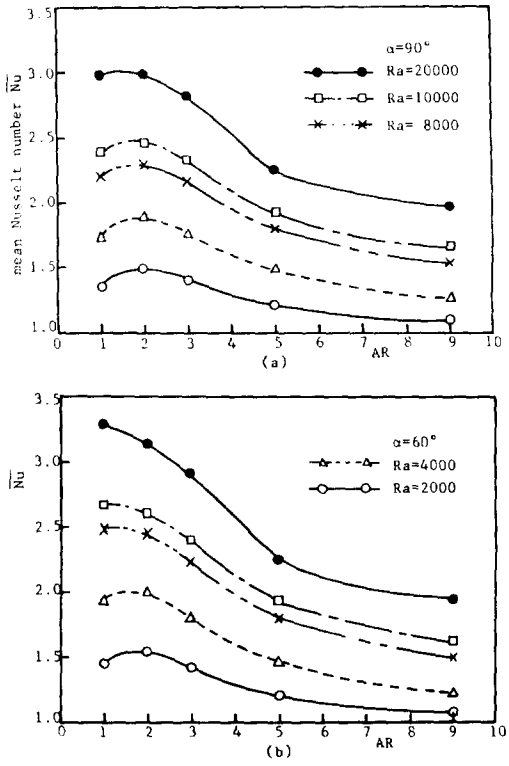

Fig. 8. Computed mean Nusselt numbers vs aspect ratios at various Rayleigh numbers : (a) $\alpha = 90°$ (b) $\alpha = 60°$ (c) $\alpha = 45°$ (d) $\alpha = 30°$

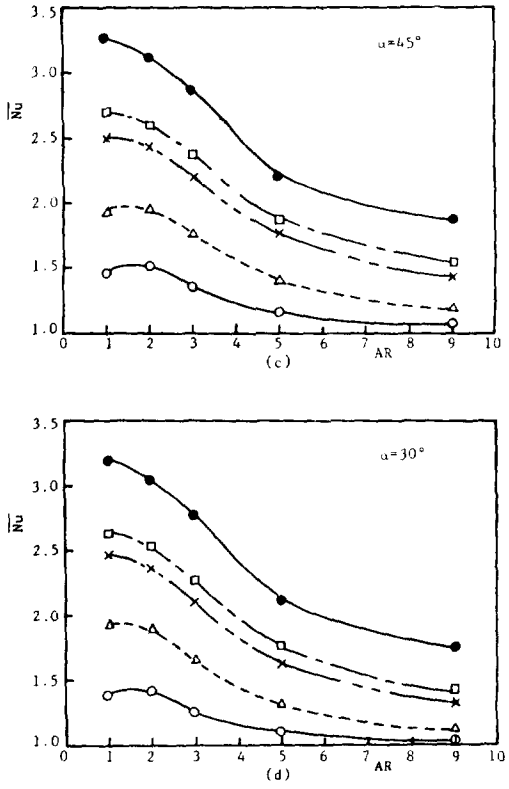

Fig. 8. (Continued.)

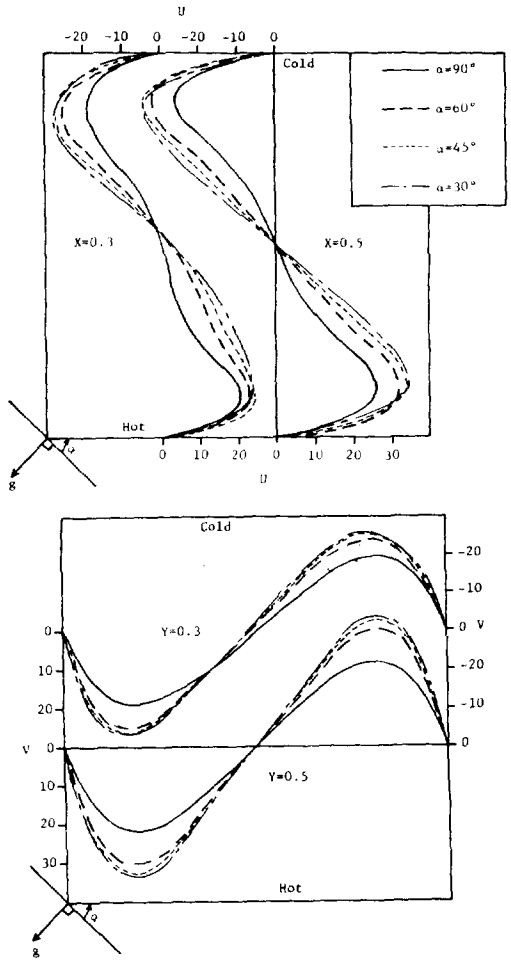

Fig. 9. Computed effect of angle of inclination on velocity field for AR= 1.0, Pr= 0.73 Ra= 1.0×10^4, $\alpha = 90°$, insulated

greater than 60 degrees. As shown in Fig. 8, the mean Nusselt number gradually decreased by the increase of aspect ratio at the various Rayleigh numbers and the angles of inclination except for the angle of inclination of 90 degrees. For the angle of inclination 90 degrees the mean Nusselt number reaches a maximum at an aspect ratio of 2.0, and then decreases as aspect ratio is further increased.

The effect of the angle of inclination on the velocity field is illustrated in Fig. 9 for Rayleigh number of 1.0×10^6, Prandtl number of 0.73, and aspect ratio of 1.0. The highest velocity is about the angle of inclination of 45 degrees which agrees with the maximum in the mean Nusselt number.

D. Isothermals and Streamlines

Perhaps the most interesting results of this study are the transient and steady state iosthermals and streamlines. Those are presented in detail in Kim [1].

VI. Conclusions

In this work heat transfer by natural convection in inclined flat plate enclosures heated from the bottom has been investigated using numerical techniques. The time dependent governing differential equations were solved using a finite difference method. Steady state solutions were obtained for the values of the Grashof number ranging from 2.74×10^3 to

2.0×10^6, for the Prandtl number of 0.73, and for aspect ratios of 1.0, 2.0, 3.0, 5.0, and 9.0. The angles of inclination of the enclosure with respect to the horizontal were 15, 30, 45, 60, 90, 120, 135, and 150 degrees. The results obtained in the oresent study are summarized as follows:

1. A finite difference technique in which the convective and diffuse terms were seperately considered was developed for the solution of simultaneous non-linear partial differential equations and proved to be effectively stable.

2. Steady state solutions were obtained in inclined enclosures maintained at a higher uniform temperature on one inclined side and at a lower uniform temperature on the opposite side. There was a good agreement between the computed values and theoretical and experimental results which were determined previously. The variation of isothermals and streamlines in transient and steady state may also be analyzed in this result.

3. Based on the results of the effect of the angle of inclination on the mean Nusselt number, the maximum value is found to be occurred at 45 degrees for aspect ratio of 1.0 and 60 degrees for aspect ratios of 2.0, 3.0, 5.0, and 9,0, respectively.

4. The Nusselt number increases with increase in the Rayleigh number, regardless of the angle of inclination. Also, as the aspect ratio increases, the mean Nusselt number decreases at various Rayleigh numbers and angles of inclination except for the angle of 90 degrees. The mean Nusselt number reaches a maximum at an aspect ratio of 2.0, and then gradually decreases as aspect ratio is further increased.

REFERENCES

1. Kim, Y.H. 1984. Numerical Analysis of Natural Convection in Inclined Flat Plate Enclosures. M.S. Thesis. Seoul National University.
2. Batchelor, G.K. 1954. Heat Transfer by Free Convection Across a Closed Cavity between Vertical Boundaries at Different Temperatures. Quart. Appl. Math. 12(3): 209-233.
3. Buchberg, H., I. Catton, and D.K. Edwards. 1976. Natural Convection in Enclosed Spaces - A Review of Applications to Solar Energy Collection. J. Heat Transfer, TRANS. ASME. 98 (5): 182-188.
4. Dropkin, D., and E. Somerscales. 1965. Heat Transfer by Natural Convection in Liquids Confined by Two Parallel Plates Which are Inclined at Various Angles with respect to the Horizontal. J. Heat Transfer, TRANS. ASME. 87(2): 77-84.
5. Hellums, J.D., and S.W. Churchill. 1962. Transient and Steady State, Free and Natural Convection, Numerical Solutions. A.I.Ch.E.J. 8(5): 690-695.
6. Hollands, K.G.T., T.E. Unny, G. Raithby., and L. Konicek. 1976. Free Convection Heat Transfer Across Inclined Air Layers. J. Heat Transfer, TRANS. ASME. 98(5): 189-193.
7. Koutsoheras, W., and W.W.S. Charters. 1977. Natural Convection Phenomena in Inclined Cells with Finite Side Walls-A Numerical Solution. Solar Energy. 19: 433-438.
8. Matrini, W.R., and S.W. Churchill. 1960. Natural Convection inside a Horizontal Cylinder. A.I.Ch. E.J. 6(2): 251-257.
9. Meyer, B.A., J.W. Mitchell, and M.M.El-Wakil. 1979. Natural Convection Heat Transfer in Moderate Aspect Ratio Enclosures. J. Heat Transfer, TRANS. ASME. 101(11): 655-659.
10. Ozoe, H., H. Sayama, and S.W. Churchill. 1974. Natural Convection in an Inclined Square Channel. Int. J. Heat Mass Transfer. 17: 401-406.
11. Ozoe, H., H. Sayama, and S.W. Churchill. 1975. Natural Convection in an Inclined Rectangular Channel at Various Aspect Ratios and Angles - Experimental Measurements. Int. J. Heat Mass Transfer. 18: 1425-1431.
12. Ozoe, H., K. Yamamoto, H. Sayama, and S.W. Churchill. 1974. Natural Circulation in an Inclined Rectangular Channel Heated on One Side and Cooled on the Opposite Side. Int. J. Heat Mass Transfer. 17: 1209-1217.

13. Ozoe, H., K. Yamamoto, H. Sayama, and S.W. Churchill. 1977. Natural Convection Patterns in a Long Inclined Rectangular Box Heated from Below. Int. J. Heat Mass Transfer. 20: 131-139.
14. Poots, G. 1958. Heat Transfer by Laminar Free Convection in Enclosed Plane Gas Layers. Quart. J. Mech. Appl. Math. 16(3): 257-273.
15. Randall, K.R., J.W. Mitchell, and M.M. El-Wakil. 1979. Natural Convection Heat Transfer Characteristics of Flat Plate Enclosures. J. Heat Transfer, TRANS. ASME. 101(2): 120-125.
16. Wilkes, J.O., and S.W. Churchill. 1966. The Finite Difference Computation of Natural Convection in a Rectangular Enclosures. A.T.Ch.E.J. 12(1): 161-166.

祝

學 位 取 得

性　　名：朱 思 選
生 年 月 日：1938年 6月 8日
勤 務 處：慶向大學校 農科大學 農業機械工學科
取得學位名：工學博士
學位授與大學：釜山大學校
學位取得年月日：1985年 2月 25日
學 位 論 文：流體粒子에 의한 2光束 레이저 Doppler 流速計의 光散亂 信號 特性에 關한 硏究